Water Air Soil Pollut (2022) 233:447
https://doi.org/10.1007/s11270-022-05919-9

Emission Characteristics of Particulate Matter from Coal-Fired Power Units with Different Load Conditions

Yujia Wu · Zhenyao Xu · Siqi Liu · Minghui Tang · Shengyong Lu

Received: 27 June 2022 / Accepted: 24 October 2022 / Published online: 2 November 2022

Abstract As an important source of electricity production in China, coal-fired power boiler still emits high concentrations of pollutants such as particulate matter (PM) due to large amounts of flue gas. In this study, filterable and condensable PM (CPM) were sampled in three coal-fired units. In particular, the effects of unit load and flue gas temperatures on organic/inorganic components of CPM were investigated. The emission concentration of total PM reached the lowest at the highest load of the coal-fired unit. CPM, especially the organic components in it, accounted for a high proportion of the total particulates emitted from three units. The representative organic components hydrocarbons and esters accounted for more than 40% of CPM from coal combustion, while the representative inorganic component SO_4^{2-} had the highest emission concentration. The emission concentration of representative organic components and most inorganic components in CPM was lowest when the temperature of coal-fired flue gas was lowest. It was noted that the effect of operating load and flue gas temperature on the distribution of organic compounds in CPM is limited when raw coal properties are similar.

Keywords Coal-fired unit · CPM · FPM · Operating load · Emission characteristics

1 Introduction

The flue gas from coal combustion in power plants are considered hazardous to the environment and human health (Pudasainee et al., 2010). They typically contain complicated compositions, including organic and inorganic chemicals, such as nitrogen oxides (NO_X), sulfur oxides (SO_X), particulate matter (PM), and polycyclic aromatic hydrocarbons, as well as multiple volatile organic pollutants (Lu et al., 2020; Sheta et al., 2019; Shi et al., 2015; Yan et al., 2016). Notably, the emission of PM from coal-fired power plants has always been the focus of environmental protection (Feng et al., 2018; Li et al., 2021). As one of the main sources of airborne PM, the total PM (TPM) emitted from coal-fired boilers consists of filterable and condensable PM (FPM and CPM) (Cano et al., 2019; Wang et al., 2021). FPM is a solid or liquid phase in coal-fired flue gas and its control technology has matured (Jung et al., 2020; Li et al., 2019; Liang et al., 2020). Currently, existing air pollution control devices (APCDs) have been able to limit the emission concentrations of FPM to less than 5 mg/Nm^3 (Zhang et al., 2021a). Nevertheless, CPM

Supplementary Information The online version contains supplementary material available at https://doi.org/10.1007/s11270-022-05919-9.

Y. Wu · Z. Xu · S. Liu · M. Tang · S. Lu (✉)
State Key Laboratory of Clean Energy Utilization, Institute for Thermal Power Engineering, Zhejiang University, Hangzhou 310027, China
e-mail: lushy@zju.edu.cn

is in the gas or vapor phase under stack conditions and it could not be directly captured by a traditional filtration or dust pelletizing system (Choi et al., 2019; Li et al., 2017b; Yang et al., 2018). Countless scientific studies have confirmed that CPM may cause haze weather, which could also contain carcinogens and present more significant risks to human health (Cano et al., 2021; Pope et al., 2019; Yang et al., 2017; Zhang et al., 2021b). However, no country has established limit regulations for CPM emissions in the world until now. Therefore, research on the impact of CPM emissions from coal combustion on the atmospheric environment and human health bears practical significance to improve air quality and formulate limit standards for CPM from representative stationary sources.

Emission characteristics, physical and chemical properties, and controlling the influencing factors of CPM are essential to assess the adverse effects on the environment and human health, as well as to develop future formulating air pollution regulations. Current research on CPM from coal combustion mainly involves its emission characteristics and main chemical compositions in actual coal-fired sources. The emission data of some representative coal-fired units in the past 5 years have shown that the CPM concentrations account for most of the TPM (43.74 ~ 90.60%) (Li et al., 2017b; Lu et al., 2019; Song et al., 2020; Wang et al., 2020b; Yang et al., 2018; Zheng et al., 2018). The existing conclusions have confirmed that the main part of the inorganic component in CPM is composed of water-soluble ions (metal cations: Na^+, Ca^{2+}, Mg^{2+}, etc.; inorganic anions: SO_4^{2-}, Cl^-, NO_3^-, etc.) (Li et al., 2017a, b; Pei, 2015; Wang et al., 2018). Moreover, the results of our past research suggested that the organic components in CPM include alkanes, esters, highly toxic polycyclic aromatic hydrocarbons, and other organic compounds, whose proportion cannot be ignored (Song et al., 2020; Wu et al., 2021a, b, c). Since APCDs cannot completely remove CPM, the effect of coal-fired units with different loads equipped with the same APCDs on CPM emissions needs to be paid enough attention to. However, this kind of conclusion has seldom been reported especially for the ultralow emission coal-fired power units that are not operating at full capacity. Emission inventories with all-sided FPM and inorganic species in CPM, as well as representative organic pollutants in CPM, are still lacking.

Under these premises, we conducted a field sampling of CPM and FPM in three coal-fired units with the same APCDs and different load conditions, which were selected at an ultralow emission power plant. The effects of actual operating load and flue gas temperature of coal-fired units on the properties of particulates were investigated through large-scale field tests. In particular, the coal-fired units selected in this study are all in a low-load operation state, which is of great reference significance for the emission of pollutants in peak load regulating the operation of power units set in the actual process.

2 Experimental Section

2.1 Facility and Sampling Sites

Three coal-fired units (e.g., unit I, unit II, and unit III) in a typical ultra-low emission power plant in China were selected to analyze the effects of unit load and flue gas temperatures on CPM and FPM from the coal burning process. Table S1 shows the proximate and ultimate analyses of the feeding coal burned by the three units. According to the coal quality data, all three kinds of coal belong to bituminous. The raw coal used in three units is all special low-sulfur coal with low ash content.

All three coal-fired units have undergone ultra-low emission modifications and are equipped with the same series of APCDs. As shown in Figure S1, the flue gas released from coal combustion passes through a selective catalytic reduction (SCR) denitration device, a low-low temperature electrostatic precipitator (LLT-ESP), a wet flue gas desulfurization (WFGD) system, and a wet electrostatic precipitator (WESP) successively, and finally is discharged into the atmosphere through the chimney. The Mitsubishi Gas–Gas Heater (MGGH) is installed between the SCR and LLT-ESP, and between the WESP and the stack to heat and cool the coal-fired flue gas, respectively, to improve the overall operating efficiency of the units and reduce pollutant emissions. Sampling sites (A, B, and C) were set up at the stacks of three units to sample CPM and FPM emitted by three coal-fired units with different loads.

Table S2 lists the distribution of sampling sites and the actual operating condition of the units. It was noted that the three units were operated at a

capacity of 40%. Of special note are the coal-fired power plant equipped with solar power devices in response to the call for national development and utilization of new energy sources. During the daytime sampling, the solar power units were in operation and the thermal power units were under load reduction. Besides, during the sampling process, the types of coal burned by each unit remained unchanged, the operating loads were stable, and the related parameters of APCDs also remained stable during the operation.

2.2 Sampling Equipment and Methods

As shown in Figure S2, a sampling system that can simultaneously collect CPM and FPM was used in this study. Depending on the properties of PM in coal-fired flue gas, CPM and FPM need to be collected separately, and the sampling method of CPM refers to EPA Method 202. The sampling system includes a portable dust direct reading instrument (ZR-7100), a heating type flue gas sampling gun (ZR-D10AT), a three-stage PM_{10} impactor (Dekati, PM_{10}-$PM_{2.5}$-PM_1), CPM collection devices (a vertical coil condenser, a short and a long knockout impactor, a filter, and connect components), a cold box (M5-CB08), and a coolant recirculating pump (M23-RC-V).

The coal-fired flue gas was sampled by the sampling tube at isokinetic speed. The mass of FPM with different particle sizes can be obtained when collected by the Dekati impactor. It is important to note that in the part of the FPM collection, both the pipe and the collection device need to maintain the heating state to prevent the early condensation of flue gas from affecting the subsequent CPM collection. Then the remaining flue gas was cooled by the condenser and entered into two knockout impactors. During the whole cooling process, CPM was captured by two impactors and the filter membrane, and the sum of the CPM collected by the three devices was the quality of CPM in the flue gas. Finally, the mass concentrations of CPM and FPM were obtained by combining the volume of coal-fired flue gas after laboratory treatment. Detailed descriptions of the process and the specific functions of the devices have been presented in previous studies (Wu et al., 2022a, b).

2.3 Analytical Procedure for Samples

2.3.1 Analytical Procedure for CPM and FPM

Particulate samples collected from the coal-fired flue gas need to be pretreated in the laboratory. The membranes that collected FPM were dried for 2 h at 50 °C and then weighed. Combined with clean membrane quality and flue gas volume, the mass concentration of FPM with different particle sizes can be obtained. For CPM, the membranes in the filter and the collected organic and inorganic lotion need to be treated separately. Previous studies (Wu et al., 2021a, b, c) and Figure S3 have described this process in detail. Similarly, the mass concentration of CPM can be obtained combined with the mass of the two components and flue gas volume. It is worth noting that the mass of the total PM is the sum of the masses of FPM and CPM.

2.3.2 Analytical Procedure for Organic and Inorganic Components in CPM

The qualitative of organic components in CPM was analyzed using a gas chromatograph/mass spectrometer (GC/MS) system (Agilent 7890B-5977A). The purpose of qualitative analysis is to determine the composition of organic compounds in CPM and provide a basis for accurate quantitative analysis of organic components. The organic components in the pretreated CPM were analyzed qualitatively, and the samples were injected with a full scan to obtain the total ion chromatogram. It was noted that due to the different response values of different organic compounds on GC/MS, the peak area ratio is only used for reference, not as a quantitative result. According to the qualitative analysis results of this experiment and the previous research and analysis (Li et al., 2017b, 2019; Song et al., 2020; Wu et al., 2021a), the *n*-alkanes and phthalates, which accounted for higher proportion and high toxicity, were selected for accurate quantitative analysis. The 19 monocomponent *n*-alkanes and 15 monocomponent phthalates in CPM were accurately quantified on GC/MS by the external standard method.

An ion chromatograph (model, Dionex ICS-2000) was used to quantify the anions (SO_4^{2-}, NO_3^-, F^-, Cl^-) and NH_4^+. Inductively coupled plasma mass spectrometry (ICP-MS, AAS, model Thermo

iCAP6300, quadrupole mass spectrometer) was used to quantitatively measure the metal elements (Na, Ca, Mg). The calibration curves should be made during the analysis of inorganic components in CPM, and the correlation coefficient (R^2) should be greater than 0.99 to ensure accuracy. Noted that due to the high concentration of water-soluble ions to be measured in the sample, the cationic sample should be diluted by 2 times and the anionic sample by 10 times before detection. The pretreatment of CPM samples and the operating parameters of GC/MS has been shown in previous studies (Wu et al., 2021a, b, c).

2.3.3 *Analytical Procedure for Organic Components in Raw Coal*

Raw coal burned during the sampling process was collected from the three coal-fired power units, then ground and dried. Detailed processing and analytical methods have been shown in Song et al.'s (2020) research. In order to facilitate the direct comparison between the concentration of organic matter in CPM and raw coal, the mass concentration (mg/Nm^3) of organic components in raw coal is calculated by the following formula:

$$C_S = \frac{M_O \times A_U \times A_F}{A_C} \quad (1)$$

where M_O (mg) is the mass of organic pollutants. A_U (kg), A_F (Nm^3/h), and A_C (kg/h) represented the amount of coal used in extracting, the amount of flue gas generated in power units, and the amount of coal used in burning, respectively.

2.4 Quality Assurance and Control

To ensure the reliability of the treatment and analysis method, the pretreatment method was verified by the recovery experiment, and the recovery rates of *n*-alkanes and phthalates were between 70 and 120%, meeting the experimental requirements. The sampling method referred to EPA Method 202 and standard ISO 23210 and has been adapted for sampling in the actual coal-fired flue gas. The minimum detection limit of the GC/MS system reached 0.288 mg/Nm^3 for organic components and 0.800 mg/Nm^3 for inorganic components in CPM. It should be noted that the standard and the test sample must be injected into the GC/MS together for analysis to reduce the experimental error. The R^2 of the nineteen *n*-alkane and fifteen phthalate standard curves were all greater than 0.99, which met the quantitative requirements.

3 Results and Discussion

3.1 Emission Characteristics of FPM and CPM from the Three Coal-Fired Units

Table 1 shows the concentrations of FPM and CPM emitted from the three units. Figure 1 shows the variation of PM emission concentrations with different particle sizes and components. By comparing units III and I or units II and I from Table 1, it can be found that with the decrease in unit loads, the emission levels of PM increase on the whole. However, the concentration of total PM emitted from units II and III was similar, and even the emission level of unit III increased slightly. It illustrates that the higher-load boiler emits a lower concentration of PM during combustion. But when the operating load exceeds the critical value of the load, the PM emission concentration increases instead as the boiler is not operating at full load. It can be speculated that before the operating load of coal-fired units reaches the critical value load, the size of the operating load is the dominant factor affecting the PM emission concentration, while beyond the critical value, the ratio of the operating load to the rated load has a greater impact on the PM

Table 1 Emission concentrations of FPM and CPM from the units (mg/Nm^3)

Unit	Condensable particulate matter			Filterable particulate matter			Total particulate matter
	Organic components	Inorganic components	Total	$FPM_{2.5}$	FPM_{10}	Total	
I	9.48	3.92	13.40	0.80	0.91	2.18	15.58
II	7.19	2.28	9.47	1.82	1.99	2.67	12.14
III	6.60	3.27	9.87	1.68	1.95	2.38	12.25

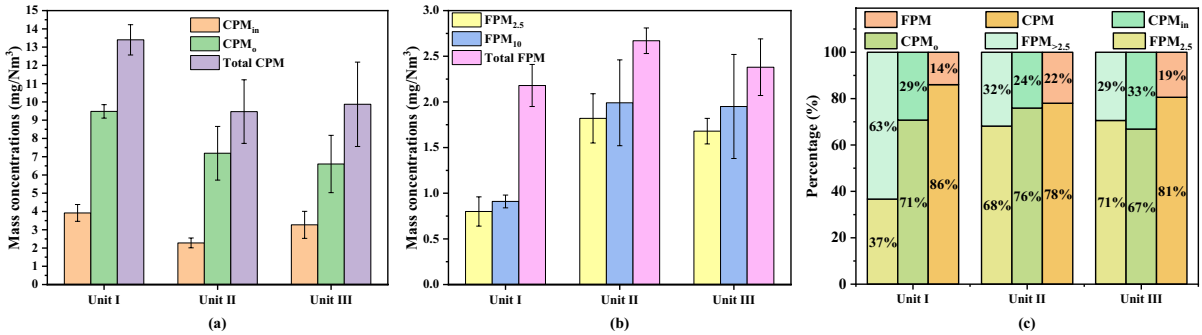

Fig. 1 **a-c** Distribution of $FPM_{>2.5}$, $FPM_{2.5}$, CPM_{in}, and CPM_{o} emitted from units with different operating load

emission concentration. It can be seen from Fig. 1a, b, among the three coal-fired units, the unit with the lowest operating load, the unit I emitted the highest CPM concentration and the lowest FPM concentration. Compared with unit I, unit II with intermediate operating load emitted lower concentrations of CPM while higher concentrations of FPM. Nevertheless, the CPM and FPM emission concentrations of unit III, the unit with the highest operating load, were higher and lower compared to unit II, respectively. In other words, when coal-fired units with the same APCDs are operated under the same percentage loads, the actual operating loads have the opposite effects on the emission concentrations of CPM and FPM. In principle, the temperature change will lead to the condensation or evaporation of CPM in coal-fired flue gas, and the realization of gas–solid phase conversion between CPM and FPM, which may become an important factor affecting its emission concentration. Figure 2 shows the effect of flue gas temperature on the emission concentration of CPM and FPM. As the temperature decreased and then increased, the change of phase state of some CPM resulted in the opposite change of FPM concentration. What is clear from the data is that the FPM emission concentrations of the three units ranged from 2.18 to 2.67 mg/Nm^3, and the concentration of FPM emitted from each coal-fired unit was lower than 5 mg/Nm^3 (even below 3 mg/Nm^3), which met the emission level requirements after the ultra-low emission transformation. Results demonstrated that the ultra-low emission retrofit of large coal-fired units can effectively control the emission concentration of FPM. It is worth noting that the proportion of $FPM_{2.5}$ emitted from the three units in FPM reached 36.7%, 68.2%, and 70.6% respectively.

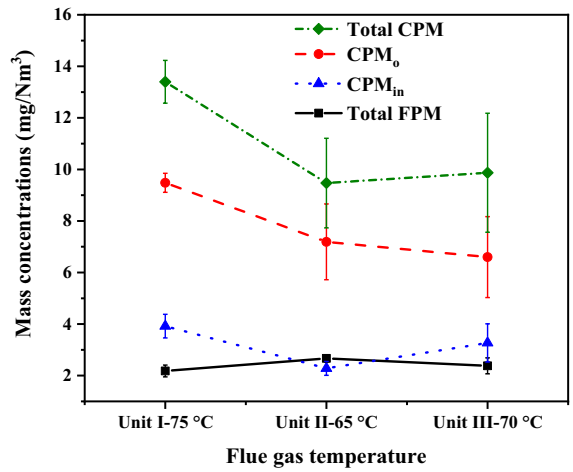

Fig. 2 The effect of flue gas temperature on the emission concentration of PM

With the increase of a load of coal-fired units, the proportion of $FPM_{2.5}$ in FPM gradually increased. It may be because the larger the unit capacity is, the more fully the coal is burned, leading to the increase in the proportion of fine particles in FPM. Combined with the previous research (Sui et al., 2016; Wu et al., 2021a; Zhang et al., 2016) on the removal effect of existing APCDs on PM, the control of fine particles during coal combustion is still the focus of future research.

Figure 1c shows that the proportion of CPM in TPM emission concentration was 86.0%, 78.0%, and 80.57% respectively, all of which were much higher than 50%. Consistent with previous studies (Cano et al., 2017; Morino et al., 2018; Yang et al., 2018), CPM has become the dominant emission

concentration of TPM from coal combustion. In addition, the emission concentrations of CPM from units are 3–6 times that of FPM, much higher than 5 mg/Nm^3. Although there is no restriction on the emission of CPM under the current standards, the CPM from coal combustion emitted into the atmosphere will cool and condense into particles to form air pollution, especially ultrafine particles (aerodynamic diameter ≤ 1.0 μm, PM_1), which will seriously harm the environment and human health. Therefore, limiting the emission of CPM is as important as limiting the emission of FPM. In order to limit the emission concentration of CPM, it is necessary to understand the specific composition of CPM. During the field sampling, the organic and inorganic components of CPM (CPM_o and CPM_{in}) were collected separately. Results show that the concentrations of organic components in CPM were higher than that of inorganic components in the flue gas emitted from the three units, which is consistent with previous studies (Li et al., 2017b; Lu et al., 2019; Song et al., 2020; Zheng et al., 2018). It can be seen from Fig. 1c that the proportion of organic components emitted from the three units in CPM reached 70.8%, 75.9%, and 66.9% respectively. Besides, CPM_o accounted for 53.9–60.8% of TPM emission levels, which demonstrated that even for TPM emissions, CPM_o still accounts for more than 50%. As shown in Fig. 2, the concentrations of CPM_{in} emitted from the three units increased with the rise of temperature, while the CPM_o decreased first and then increased with the rise of temperature, indicating that the flue gas temperature had a greater impact on CPM_{in}. Nevertheless, the CPM_o may also be affected by other factors such as pressure, and the influence of temperature on the CPM_o needs further study. Therefore, it is necessary to study the organic components of CPM from coal combustion. A full understanding of the organic composition of CPM and the factors affecting the change of its concentration can help to reduce the emission of TPM.

3.2 Components' Analysis of CPM Emitted from the Three Coal-Fired Units

Figure 3 shows the distribution proportion of organic components in CPM emitted from the three units. What is clear is that the changes in a load of different coal-fired units have little effect on the proportion of organic components in CPM. That is, the CPM produced from the coal burning process has a similar composition of organic components after being purified by the same APCDs. Hydrocarbons are the highest proportion of organic components, and the percentages of CPM_o emitted from the three units are relatively stable, reaching 29–31%. According to the results of this study and previous data on coal-fired industrial boilers (Wu et al., 2021a, b), almost all hydrocarbons in CPM_o are saturated hydrocarbons, such as *n*-alkanes and isoparaffins. In addition, the hydrocarbon organics in CPM_o also include very small amounts of unsaturated hydrocarbons, alicyclic hydrocarbons, and aromatic hydrocarbons. As shown in Fig. 3, there were still a relatively high proportion of oxygen-containing derivatives represented by esters in CPM_o. The proportion of esters in CPM_o emitted from the three coal-fired units all exceeded

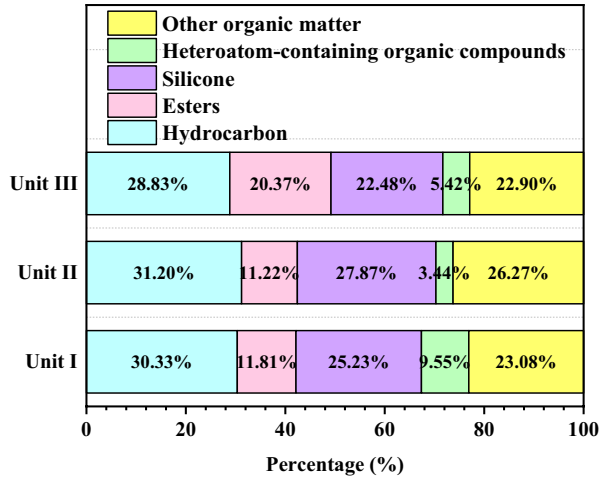

Fig. 3 Distribution percentage of organic matter in CPM from coal-fired units

10%. Results demonstrated that phthalic acid esters and fatty acid methyl esters are representative of ester organics in CPM_o. Besides, a small amount of eicosyl acetate, ethyl geranyl acetate, etc. was also detected in the organic components of CPM. What is noteworthy is that the proportions of silicone in CPM_o reached 22 ~ 28%, which needs to be paid attention to. The detected silicone included heptasiloxane, octasiloxane, and so on. Other organics detected in CPM include halohydrocarbon, alcohols, phenols, ethers, aldehydes, ketones, and carboxylic acids. In addition to organics containing only the three elements of carbon, hydrogen, and oxygen, there were also some heteroatom-containing organics containing sulfur, nitrogen, and halogen. Li et al. (2017b) found that there were dozens of organics in CPM_o discharged in the process of coal burning, some of which were highly toxic and potentially harmful to the human body and environment. In summary, the emission concentrations of organic components in CPM produced from coal combustion are low, but the composition is complex, the total amount is large, and the toxicity is high. Therefore, attention should be paid to the exploration of its formation mechanism and the development of corresponding control methods. Furthermore, this study contributed some useful basic data on the composition of the organic fraction in CPM.

As shown in Fig. 4, the concentrations of four anions, SO_4^{2-}, Cl^-, NO_3^-, and F^-, three metal cations, Ca^{2+}, Na^+, and Mg^{2+}, and NH_4^+ in CPM_{in} were accurately quantified. The mass concentrations of total inorganic components in the CPM emitted from three coal-fired power units were 3.92, 2.28, and 3.27 mg/Nm^3. Figure 4a shows that the SO_4^{2-} was the most abundant species that accounted for 31.38%, 57.46%, and 41.59% in the CPM_{in}, and other detected water-soluble ions only accounted for relatively small amounts, which confirmed the previous research results (Guo et al., 2006; Yang et al., 2015). The concentrations of Cl^- in CPM_{in} from coal combustion were 0.51, 0.24, and 0.71 mg/Nm^3 respectively, second only to SO_4^{2-}, and Cl^- mainly came from HCl which was produced by the combustion and gasification of highly volatile chlorine in coal (Deng et al., 2014; Feng et al., 2021). The concentrations of NO_3^- were even lower in the inorganic components, which might be attributed to the absorption of HNO_3 and nitrates in the coal-fired flue gas. Moreover, the concentrations of F^- in CPM_{in} were almost

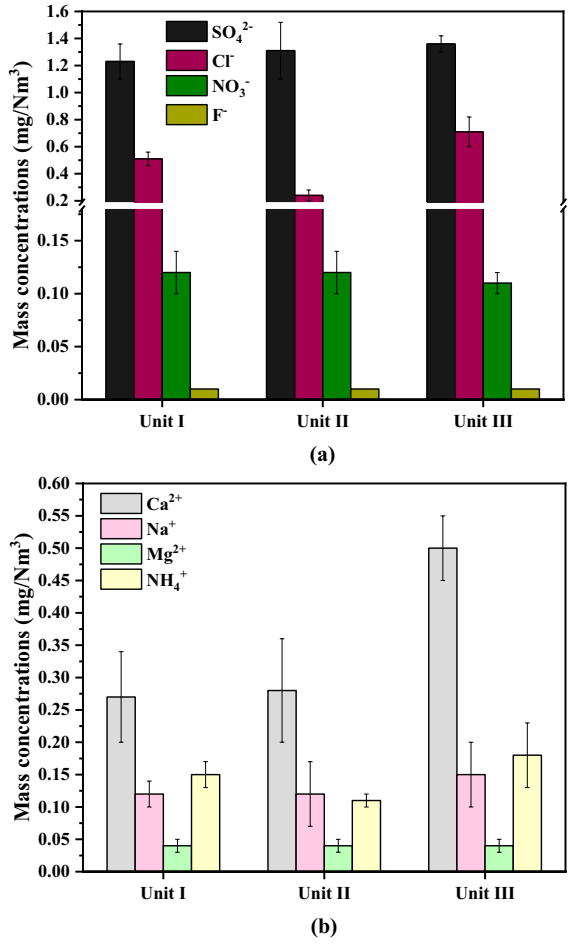

Fig. 4 The emission concentration of inorganic anions (**a**) and metal cations (**b**) in CPM from units

negligible. For metal cations in Fig. 4b, the concentrations of Ca^{2+} in CPM_{in} were the highest, reaching 0.27–0.50 mg/Nm^3, while the concentrations of Mg^{2+} were the lowest, not exceeding 0.05 mg/Nm^3. The presence of Ca^{2+} and Mg^{2+} in the detected results was probably due to some aerosols generated in the WFGD scrubber were too tiny to be collected by the FPM filter (Huang et al., 2020). The concentrations of Na^+ in CPM_{in} were slightly higher than that of Mg^{2+}. It is probably due to the reason that Na^+ in CPM_{in} might be attributed to the absorption of sodium salts in the coal-fired flue gas (Wang et al., 2020a). It was noted that NH_4^+ was considered to be the main ionic component in water-soluble ion emissions from coal-fired power plants (Guo et al., 2006; Hu et al., 2015). In this research, the average concentration of

NH_4^+ in CPM_{in} emitted from three coal-fired units was 0.15 mg/Nm^3. According to the study by Feng et al. (2021) NH_4^+ in CPM_{in} might derive from NH_3 that reacted with acid gases to form ammonium compounds, such as ammonium salts, which became a part of the inorganic components in CPM during the cooling process of the coal-fired flue gas. Similar results (Feng et al., 2020; Wang et al., 2014) have shown that water-soluble ions, such as SO_4^{2-}, NO_3^-, and NH_4^+, are the main ionic components in atmospheric $PM_{2.5}$ around combustion sources, thereby revealing that CPM_{in} emitted from coal-fired power units may significantly affect the water-soluble ions in atmospheric $PM_{2.5}$. As a result, the precise quantification and emission control of the inorganic fraction in CPM from large coal-fired power plants bear practical significance.

3.3 Analysis of Representative Organic Components in CPM

The qualitative analysis results of organic components in CPM in the previous chapter showed that hydrocarbons, esters, and silicone accounted for a large proportion. However, the precise quantitative method of silicone in CPM is still in the process of exploration. In this study, *n*-alkanes and phthalate were selected as the representative organics in the hydrocarbons and esters in CPM from coal combustion for accurate quantitative analysis. The emission concentrations of two types of monocomponent organic compounds from coal-fired units under different operating conditions were studied and the factors affecting the emissions were discussed.

3.3.1 Quantitative Analysis of n-Alkanes in CPM and Raw Coal

Figures 5 and 6 show the concentrations of 18 (C_{16}~C_{33}) and 19 (C_{16}~C_{34}) *n*-alkanes detected in raw coal and CPM emitted from coal combustion, respectively. It is observed that the concentrations of *n*-alkanes in CPM emitted from the three units with different operating conditions increased firstly and then decreased with the increase of loads. Similar to the effect of flue gas temperature, the changing trend of CPM concentrations and *n*-alkane concentrations was consistent. It can be found in Fig. 6 that the distribution of monocomponent *n*-alkanes in CPM discharged by the three units was similar, showing a trend of increasing first and then decreasing, and the main peak carbon all appears near C_{27}, presenting a typical single-peak distribution. Slightly different from the previous results of Song et al.'s (2020) study, CPM was detected in the flue gas of the entire purification process of coal-fired power plants. The conclusions from the research showed that the concentration distribution of *n*-alkanes with different carbon numbers in CPM was similar to the Gaussian distribution. It was noted that the concentration of *n*-alkanes in the main peak carbon was the highest,

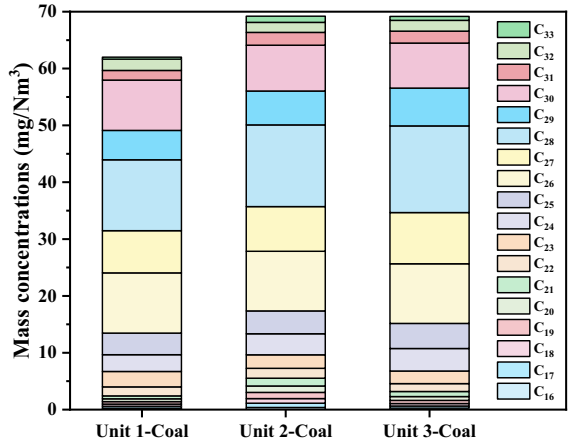

Fig. 5 Distribution characteristics of *n*-alkanes in raw coal from units

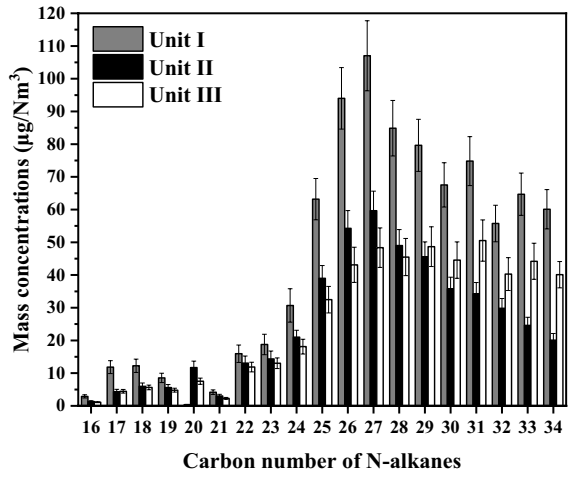

Fig. 6 Distribution of monocomponent *n*-alkanes in CPM from coal-fired units

and the concentrations of *n*-alkanes far away from the main peak carbon decreased sequentially. However, in this study, the concentrations of *n*-alkanes in CPM were in a downward trend after the main peak carbon, but they still maintained high emission levels. It is speculated that this may be related to the occurrence and distribution of *n*-alkanes in raw coal, so the concentration of *n*-alkanes in raw coal was quantitatively analyzed.

As shown in Fig. 5, the concentrations of *n*-alkanes in the raw coal were 78 ~ 153 times the concentrations of *n*-alkanes in CPM in the exhaust coal-fired flue gas. According to previous research results (Li et al., 2021; Song et al., 2020), part of the *n*-alkanes that occurred in coal could be removed by the process of burning, especially the components with lower melting points. In addition, the existing APCDs installed in the units have been shown to promote the purification of *n*-alkanes from coal combustion. Figure 5 also shows that the concentrations of *n*-alkanes occurring in raw coal first increased and then decreased with the increase of carbon number, reaching the highest at C_{26} ~ C_{30}, and the concentrations of *n*-alkanes with higher carbon numbers were relatively high. The difference was that after the process of combustion, the content of small-molecule *n*-alkanes, that is, *n*-alkanes with fewer carbons in the CPM, was greatly reduced. It can be inferred that the organic matter that occurred in the raw coal may have a certain influence on the concentration of the organic components in CPM from coal combustion. In general, in the context of clean utilization of coal, not only the sulfur content, volatile content, and other parameters involved in the elemental analysis and proximate analysis of coal should be considered, but also the organic pollutants in raw coal should be detected, and various factors should be considered comprehensively to select coal with better quality.

The emission concentrations of *n*-alkanes in the CPM of the three coal-fired units accounted for 8.41%, 6.29%, and 7.07% of the CPM_o, respectively. Significantly, as shown in Fig. 6, *n*-alkanes with lower carbon numbers (C_{16} ~ C_{26}) accounted for less than 40% of the total concentration, while *n*-alkanes with more than 27 carbons (C_{27} ~ C_{34}) make a significant contribution to the total concentration. One possible reason is that *n*-alkanes with smaller relative molecular masses are easier to decompose during the combustion process (Liu et al., 2003), resulting in a lower emission concentration of small molecules of *n*-alkanes in the flue gas. The other lies in the *n*-alkanes with more carbons have higher melting and boiling points, which are easier to condense and be collected in the cooling sampling process, resulting in a larger proportion of *n*-alkanes with more carbons in CPM. In addition, it should be noted that the distribution proportion of large-molecule *n*-alkanes in raw coal was also higher than that of small-molecule *n*-alkanes. Therefore, it is very important to select the appropriate coal species for the emission control of representative organic pollutants. In general, for different coal-fired power units with the same flue gas purification process and similar coal, the distribution proportions of monocomponent *n*-alkanes in the flue gas emitted from coal combustion are similar. This similarity of organic matter distribution is conducive to the targeted reduction of *n*-alkane emissions in CPM, that is, to reduce the total emission concentration of *n*-alkanes by reducing the concentration of peak *n*-alkanes, which is of great significance for the realization of clean coal combustion.

3.3.2 Quantitative Analysis of Phthalates in CPM and Raw Coal

Figures 7 and 8 show the concentrations of 15 phthalates detected in raw coal and CPM emitted from coal combustion, respectively. It can be found that the total concentration of phthalates in CPM emitted from the three coal-fired units was 146.38,

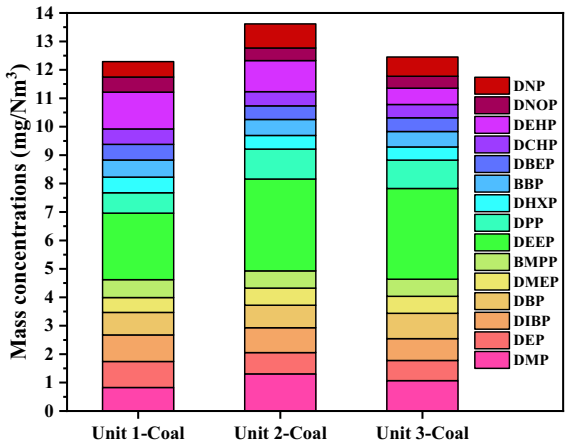

Fig. 7 Distribution characteristics of phthalates in raw coal from units

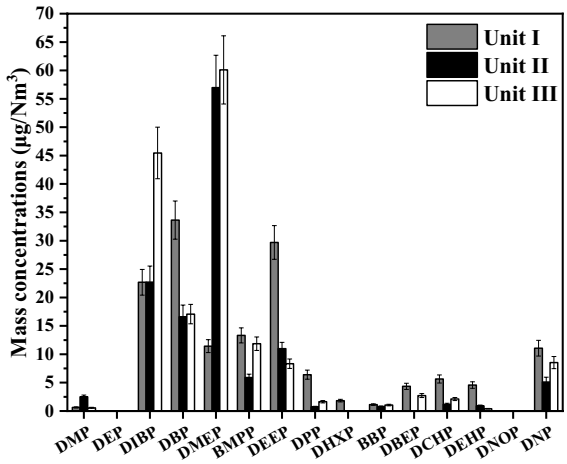

Fig. 8 Distribution of monocomponent phthalates in CPM from coal-fired units

124.31, and 159.87 μg/Nm^3, accounting for 1.54%, 1.73%, and 2.42% of CPM_o respectively, which was lower than the proportion of *n*-alkanes in CPM_o. It is worth noting that temperature had a similar effect on the distribution of phthalates and *n*-alkanes in CPM, and the concentration of phthalates in CPM of coal-fired units with the lowest flue gas temperature was the lowest. However, the distribution regularities of 15 kinds of monocomponent phthalates in CPM were not obvious. Among them, 4 kinds of phthalates (DEP, DHXP, DBEP, and DNOP) were not detected in the CPM of flue gas discharged under some working conditions, while 5 kinds of phthalates (DIBP, DBP, DMEP, BMPP, and DEEP) almost contributed to the total emission concentration. It can be concluded that in order to reduce the emission concentration of phthalates in CPM, it is necessary to selectively control the emission of monocomponent organic matter which accounts for a large proportion. It can be also found in Fig. 7 that except for DEEP, the distribution proportion of other monocomponent phthalates was relatively uniform. According to the existing test results, there is no obvious correlation between the distribution of phthalates in raw coal and that in CPM emitted from the stacks. This conclusion still needs a lot of basic data from the field and laboratory to verify.

4 Conclusions

Condensable and filterable particulate matter in coal-fired flue gas from three power units installed with the same types of APCDs was sampled. This study explored the effect of unit loads on the emission of CPM and FPM from coal combustion. The analysis results can be summarized as follows: (1) CPM contributed the main part of total PM emission concentration, accounting for 86.01%, 78.01%, and 80.57% of flue gas emitted from the three coal-fired units, respectively. Organic components were the main fraction of CPM, accounting for 66.87 to 75.92% of CPM discharged by the three units. (2) CPM had a similar composition of organic components emitted from the coal-fired power units with the same APCDs under different operating loads. Hydrocarbons were the highest proportion (29 ~ 31%) of organic components in CPM, and the percentages of esters all exceeded 10%. The SO_4^{2-} was the highest concentration of water-soluble ions that accounted for 31.38 to 57.46% of the inorganic components in CPM. (3) For *n*-alkanes of organic in CPM emitted from the three coal-fired units, the distribution characteristics of monocomponent *n*-alkanes were similar. For phthalates, 5 kinds of phthalates, that is, DIBP, DBP, DMEP, BMPP, and DEEP, almost contributed to the total emission concentration. (4) The higher-load coal-fired boiler emitted a lower concentration of TPM during combustion, and the actual operating loads had the opposite effects on the emission concentrations of CPM and FPM. With the decrease in flue gas temperature, the emission concentration of CPM also decreased, and the emission concentration of representative organic components and most inorganic components in CPM reached the lowest at the lowest temperature.

Funding The research was supported by the National Key Research and Development Program of China (2018YFB0605200).

Data Availability The datasets generated and analyzed during the current study are available from the corresponding author on reasonable request.

Declarations

Conflict of Interest The authors declare no competing interests.

References

Cano, M., Reina, T. R., Portillo, E., Gallego Fernández, L. M., & Navarrete, B. (2021). Characterization of emissions of condensable particulate matter under real operation conditions in cement clinker kilns using complementary experimental techniques. *Science of the Total Environment, 786*, 147472.

Cano, M., Vega, F., Navarrete, B., Plumed, A., & Camino, J. A. (2017). Characterization of emissions of condensable particulate matter in clinker kilns using a dilution sampling system. *Energy & Fuels, 31*, 7831–7838.

Cano, M., Vega, F., Palomo, D., Serrano, J., & Navarrete, B. (2019). Characterization of condensable particulate matter emissions in agricultural diesel engines using a dilution-based sampling train. *Energy & Fuels, 33*, 779–787.

Choi, D. S., Kim, Y.-M., Lee, I. H., Jeon, K.-J., Choi, B. J., & Park, Y.-K. (2019). Study on the contribution ratios of particulate matter emissions in differential provinces concerning condensable particulate matter. *Energy & Environment (Essex England), 30*, 1206–1218.

Deng, S., Zhang, C., Liu, Y., Cao, Q., Xu, Y.-Y., Wang, H.-L., & Zhang, F. (2014). A full-scale field study on chlorine emission of pulverized coal-fired power plants in China. *Research Environmental Science, 27*, 127–133.

Feng, Y., Li, Y., & Cui, L. (2018). Critical review of condensable particulate matter. *Fuel, 224*, 801–813.

Feng, Y., Li, Y., Zhang, X., Su, S., Zhang, Z., Gan, Z., & Dong, Y. (2021). Comparative study on the characteristics of condensable particulate matter emitted from three kinds of coal. *Environmental Pollution (1987), 270*, 116267.

Feng, Y., Li, Y., Zhang, X., Zhang, Z., Dong, Y., & Ma, C. (2020). Characteristics of condensable particulate matter discharging from a one-dimensional flame furnace firing lignite. *Fuel (guildford), 277*, 118198.

Guo, X., Hao, J., Duan, L., Yi, H., & Li, X. (2006). Characteristics of water soluble ions emitted from large coal-fired power plant boilers. *Journal of Tsinghua University (Sci & Tech), 046*, 1991–1994.

Hu, Y.-Q., Ma, Z.-H., Feng, Y.-J., Wang, C., Chen, Y.-Y., & He, M. (2015). Emission characteristics of water-soluble ions in fumes of coal fired boilers in Beijing. *Environmental Science, 36*, 1966–1974.

Huang, R., Wu, H., & Yang, L. (2020). Investigation on condensable particulate matter emission characteristics in wet ammonia-based desulfurization system. *Journal of Environmental Sciences (china), 92*, 95–105.

Jung, W., Jeong, M. H., Ahn, K. H., Kim, T., & Kim, Y. H. (2020). Reduced graphene-oxide filter system for removing filterable and condensable particulate matter from source. *Journal of Hazardous Materials, 391*, 122223.

Li, J., Li, X., Wang, W., Wang, X., Lu, S., Sun, J., & Mao, Y. (2021). Investigation on removal effects and condensation characteristics of condensable particulate matter: Field test and experimental study. *Science of the Total Environment, 783*, 146985.

Li, J., Li, X., Zhou, C., Li, M., Lu, S., Yan, J., & Qi, Z. (2017a). Study on the influencing factors of the distribution characteristics of polycyclic aromatic hydrocarbons in condensable particulate matter. *Energy & Fuels, 31*, 13233–13238.

Li, J., Qi, Z., Li, M., Wu, D., Zhou, C., Lu, S., Yan, J., & Li, X. (2017b). Physical and chemical characteristics of condensable particulate matter from an ultralow-emission coal-fired power plant. *Energy & Fuels, 31*, 1778–1785.

Li, X., Zhou, C., Li, J., Lu, S., & Yan, J. (2019). Distribution and emission characteristics of filterable and condensable particulate matter before and after a low-low temperature electrostatic precipitator. *Environmental Science and Pollution Research, 26*, 12798–12806.

Liang, Y., Li, Q., Ding, X., Wu, D., Wang, F., Otsuki, T., Cheng, Y., Shen, T., Li, S., & Chen, J. (2020). Forward ultra-low emission for power plants via wet electrostatic precipitators and newly developed demisters: Filterable and condensable particulate matters. *Atmospheric Environment (1994), 225*, 117372.

Liu, H., Sun, Z., Sun, J., & Yao, Q. (2003). An investigation on the characteristics of the discharge of normal paraffin organic compounds during a coal-burning process and their related formationevolution mechanism. *Journal of Engineering for Thermal Energy and Power, 18*, 36–38.

Lu, C. M., Dat, N. D., Lien, C. K., Chi, K. H., & Chang, M. B. (2019). Characteristics of fine particulate matter and polycyclic aromatic hydrocarbons emitted from coal combustion processes. *Energy & Fuels, 33*, 10247–10254.

Lu, S., Wu, Y., Chen, T., Song, J., Xu, Z., Tang, M., & Ding, S. (2020). Influence of the combination system of wet flue gas desulfurization and a wet electrostatic precipitator on the distribution of polycyclic aromatic hydrocarbons in flue gas from a coal-fired industrial plant. *Energy & Fuels, 34*, 5707–5714.

Morino, Y., Chatani, S., Tanabe, K., Fujitani, Y., Morikawa, T., Takahashi, K., Sato, K., & Sugata, S. (2018). Contributions of condensable particulate matter to atmospheric organic aerosol over Japan. *Environmental Science & Technology, 52*, 8456–8466.

Pei, B. (2015). Determination and emission of condensable particulate matter from coal-fired power plants. *Huanjing Kexue/environmental Science, 36*, 1544–1549.

Pope, C. A., Lefler, J. S., Ezzati, M., Higbee, J. D., Marshall, J. D., Kim, S.-Y., Bechle, M., Gilliat, K. S., Vernon, S. E., Robinson, A. L., & Burnett, R. T. (2019). Erratum: Mortality risk and fine particulate air pollution in a large, representative cohort of U.S. *Environmental Health Perspectives, 127*, 99002.

Pudasainee, D., Kim, J. H., Lee, S. H., Park, J. M., Jang, H. N., Song, G. J., & Seo, Y. C. (2010). Hazardous air pollutants emission from coal and oil-fired power plants. *Asia-Pacific Journal of Chemical Engineering, 5*, 299–303.

Sheta, S., Afgan, M. S., Hou, Z., Yao, S.-C., Zhang, L., Li, Z., & Wang, Z. (2019). Coal analysis by laser-induced breakdown spectroscopy: A tutorial review. *Journal of Analytical Atomic Spectrometry, 34*, 147–182.

Shi, J., Deng, H., Bai, Z., Kong, S., Wang, X., Hao, J., Han, X., & Ning, P. (2015). Emission and profile characteristic of volatile organic compounds emitted from coke production, iron smelt, heating station and power plant in Liaoning Province China. *Science of the Total Environment, 515–516*, 101–108.

Song, J., Lu, S., Wu, Y., Zhou, C., Li, X., & Li, J. (2020). Migration and distribution characteristics of organic and inorganic fractions in condensable particulate matter

emitted from an ultralow emission coal-fired power plant. *Chemosphere, 243*, 125346.

Sui, Z., Zhang, Y., Peng, Y., Norris, P., Cao, Y., & Pan, W.-P. (2016). Fine particulate matter emission and size distribution characteristics in an ultra-low emission power plant. *Fuel, 185*, 863–871.

Wang, G., Deng, J., Ma, Z., Hao, J., & Jiang, J. (2018). Characteristics of filterable and condensable particulate matter emitted from two waste incineration power plants in China. *Science of the Total Environment, 639*, 695–704.

Wang, G., Deng, J. G., Zhang, Y., Li, Y. J., Ma, Z. Z., Hao, J. M., & Jiang, J. K. (2020a). Evaluating airborne condensable particulate matter measurement methods in typical stationary sources in China. *Environmental Science & Technology, 54*, 1363–1371.

Wang, K., Jia, L., Huang, L., Cui, C., Wang, F., LÜ, N., & Zhao, Q. (2014). Pollution characteristics of water-soluble ions in $PM_{2.5}$ and PM_{10} under severe haze days. *Journal of Harbin Institute of Technology, 46*, 53–58.

Wang, K., Yang, L., Li, J., Sheng, Z., He, Q., & Wu, K. (2020b). Characteristics of condensable particulate matter before and after wet flue gas desulfurization and wet electrostatic precipitator from ultra-low emission coal-fired power plants in China. *Fuel (guildford), 278*, 118206.

Wang, L., Wu, H., Wang, Q., Zhou, C., Zhang, Z., Yang, H., & Zhou, Y. (2021). Emission reduction of condensable particulate matter in ammonia-based desulfurized flue gas by heterogeneous vapor condensation. *Chemical Engineering and Processing, 167*, 108519.

Wu, Y., Xu, Z., Huang, X., Liu, S., Tang, M., & Lu, S. (2022a). A typical 300 MW ultralow emission coal-fired power plant: Source, distribution, emission, and control of polycyclic aromatic hydrocarbons. *Fuel (Guildford), 326*, 125052

Wu, Y., Xu, Z., Liu, S., Tang, M., & Lu, S. (2021). Emission characteristics of $PM_{2.5}$ and components of condensable particulate matter from coal-fired industrial plants. *Science of the Total Environment, 796*, 148782.

Wu, Y., Xu, Z., Liu, S., Tang, M., & Lu, S. (2021). Emission of organic components and distribution characteristics of PAHs in condensable particulate matter from coal-fired power and industrial plants. *Journal of the Energy Institute, 97*, 109–116.

Wu, Y., Xu, Z., Liu, S., Tang, M., & Lu, S. (2021). Migration and emission characteristics of N-alkanes and phthalates in condensable particulate matter from coal-fired sources. *Journal of Cleaner Production, 305*, 127203.

Wu, Y., Xu, Z., Liu, S., Tang, M., & Lu, S. (2022b). Effects of the changes of load and flue gas temperature on the emission of particulate matter from the coal-fired unit. *Aerosol and Air Quality Research, 22*, 210268.

Yan, Y., Yang, C., Peng, L., Li, R., & Bai, H. (2016). Emission characteristics of volatile organic compounds from coal-, coal gangue-, and biomass-fired power plants in China. *Atmospheric Environment* (1994), 143:261–269

Yang, H.-H., Arafath, S. M., Lee, K.-T., Hsieh, Y.-S., & Han, Y.-T. (2018). Chemical characteristics of filterable and condensable $PM_{2.5}$ emissions from industrial boilers with five different fuels. *Fuel, 232*, 415–422.

Yang, H.-H., Lee, K.-T., Hsieh, Y.-S., Luo, S.-W., & Huang, R.-J. (2015). Emission characteristics and chemical compositions of both filterable and condensable fine particulate from steel plants. *Aerosol and Air Quality Research, 15*, 1672–1680.

Yang, Z., Zheng, C., Zhang, X., Li, C., Wang, Y., Weng, W., & Gao, X. (2017). Sulfuric acid aerosol formation and collection by corona discharge in a wet electrostatic precipitator. *Energy & Fuels, 31*, 8400–8406.

Zhang, J., Zheng, C., Zhang, Y., Wu, G., Zhu, S., Meng, W., Gao, X., & Cen, K. (2016). Experimental investigation of ultra-low pollutants emission characteristics from a 1 000 MW coal-fired power plant. *Proceedings of the Chinese Society for Electrical Engineering, 36*, 1310–1314.

Zhang, X., Li, Y., Zhang, Z., Nie, M., Wang, L., & Zhang, H. (2021a). Adsorption of condensable particulate matter from coal-fired flue gas by activated carbon. *Science of the Total Environment, 778*, 146245.

Zhang, Z., Li, Y., Zhang, X., Zhang, H., & Wang, L. (2021b). Review of hazardous materials in condensable particulate matter. *Fuel Processing Technology, 220*, 106892.

Zheng, C., Hong, Y., Liu, S., Yang, Z., Chang, Q., Zhang, Y., & Gao, X. (2018). Removal and emission characteristics of condensable particulate matter in an ultralow emission power plant. *Energy & Fuels, 32*, 10586–10594.